Enzymatic Regeneration of ATP

ROBERT S. LANGER
COLIN R. GARDNER
BRUCE K. HAMILTON
and
CLARK K. COLTON

Department of Chemical Engineering
Massachusetts Institute of Technology
Cambridge, Massachusetts 02139

II. Equilibrium Studies with Acetate Kinase and Adenylate Kinase

Equilibria of reactions catalyzed by acetate kinase and adenylate kinase were studied experimentally and theoretically. Nucleotide conversions in excess of 90% were obtained with reactants (acetyl phosphate and one nucleotide) in stoichiometric proportion for ATP regeneration from either ADP via acetate kinase or AMP via the coupled enzyme system. Observed equilibrium constants, measured as a function of $[Mg^{2+}]$ at pH 7.4, ranged from about 1 to 9 for the reaction catalyzed by adenylate kinase and from about 50 to 400 for the reaction catalyzed by acetate kinase. These results agreed well with prediction of a theoretical model for the multiple equilibria between all species present in solution. Theoretical calculations showed that magnesium ion complexes and totally dissociated anions are the predominant species in solution at $p\text{H} \gtrsim 7$ and $[Mg^{2+}] \gtrsim 10^{-3}$ M.

SCOPE

Prospects for cell free enzyme catalyzed syntheses on an industrial scale depend upon development of a practical process for regenerating adenosine 5′-triphosphate (ATP) from adenosine 5′-diphosphate (ADP) or adenosine 5′-monophosphate (AMP). A promising enzymatic route involves two reactions catalyzed by phosphotransferases

$$\text{AMP} + \text{ATP} \underset{\text{Kinase}}{\overset{\text{Adenylate}}{\rightleftharpoons}} 2\,\text{ADP} \qquad (1)$$

$$\text{ADP} + \text{AcP} \underset{\text{Kinase}}{\overset{\text{Acetate}}{\rightleftharpoons}} \text{ATP} + \text{Ac} \qquad (2)$$

where acetyl phosphate (AcP) is the ultimate phosphate donor, and acetate (Ac) is the by-product. Both enzymes require a divalent cation (preferably Mg^{2+}) for activity. Reaction (2) suffices for regeneration from ADP; both reactions are required for regeneration from AMP.

In this paper we report equilibrium studies of reactions (1) and (2). Assays were developed to measure the concentration of each individual reactant and product in the presence of all other components and both enzymes. Observed equilibrium constants were measured for each reaction at pH 7.4 for $10^{-5} < [Mg^{2+}] < 1$ M. Additional variables investigated with adenylate kinase included pH (6.4 and 8.4), the presence of very high total adenosine and sodium ion concentrations, and the use of different buffers or unbuffered solutions. The pH values at which experiments were conducted were selected to fall within the range where the enzymes retained substantial catalytic activity. The equilibrium composition of nucleotides was measured for ATP regeneration from AMP or ADP at pH 7.4 with the total concentrations of adenosine and magnesium held constant while acetyl phosphate concentration was varied.

Under typical reaction conditions, each component may exist in a variety of forms, including totally dissociated anions, partially protonated species, divalent metal ion (Mg^{2+}) complexes, and, under certain conditions, monovalent metal ion complexes. Reactions (1) and (2) therefore constitute a complicated network of reactions among a large variety of species, none of which is individually accessible to direct concentration measurement. A theoretical model is presented for the multiple equilibria between individual species; it permits calculation of the equilibrium composition given an arbitrary feed to a reactor. In developing the model it was necessary to determine which species should be incorporated and to select from the literature a consistent set of stability and ionization constants which gave good agreement between prediction and data.

Correspondence concerning this paper should be addressed to C. K. Colton. R. S. Langer is with the Children's Hospital Medical Center, Boston, Massachusetts. C. R. Gardner is with the Centre de Recherche Merrell International, Strasbourg, France. B. K. Hamilton is with the Frederick Cancer Research Center, Frederick, Maryland.

CONCLUSIONS AND SIGNIFICANCE

Measured values of observed equilibrium constants ranged from about 1 to 9 for adenylate kinase and from about 50 to 400 for acetate kinase. Stability and ionization constants were selected to minimize the average deviation between prediction and data for adenylate kinase, and an equilibrium parameter was fitted to the data for acetate kinase. The resulting prediction agreed well with data at all values of pH and $[Mg^{2+}]$, except for $[Mg^{2+}] > 0.1$ M. Although the activity of each species was taken to be equal to its concentration, theoretical prediction agreed excellently with experimental data over an ionic strength range of about 0.1 to 1.6.

Conversions of AMP and ADP to ATP were in excess of 90% with reactants in stoichiometric proportion and greater than 99% with a 50% molar excess of AcP, as predicted. Nucleotide conversion to ATP was predicted to be maximized for $[Mg^{2+}] \gtrsim 10^{-2}$ M.

The model was used to calculate the distribution of individual species at pH 7.4 as a function of $[Mg^{2+}]$. Totally dissociated anions and magnesium ion complexes predominate for $[Mg^{2+}] > 10^{-3}$ M. Protonated species are significant only at lower pH. In addition to its utility for predicting equilibrium composition of a reaction system for ATP regeneration, the model presented here will be of great value for calculation of individual species concentrations in the analysis of kinetic data from acetate kinase, adenylate kinase, and related enzymes.

BACKGROUND

We have previously identified the reactions catalyzed by adenylate kinase and acetate kinase as a promising enzymatic route to ATP regeneration (Langer et al., 1976). As a first step towards the development of an ATP regeneration process, we have studied the equilibrium behavior of the two reactions, singly and coupled together.

Observed equilibrium constants for reactions (1) and (2) are defined by

$$K_{1obs} = \frac{[ADP]^2}{[AMP][ATP]} \tag{3}$$

$$K_{2obs} = \frac{[ATP][Ac]}{[ADP][AcP]} \tag{4}$$

where each bracketed quantity represents total concentration of the indicated component in all forms, a variable which is experimentally measurable. Since each quantity is the sum of concentrations of ionized and complexed species, none of which are directly measurable, K_{1obs} and K_{2obs} depend upon ionic strength and the specific composition of the reaction medium, as well as temperature and pressure.

Bowen and Kerwin (1956) first reported that K_{1obs} varied substantially with $[Mg^{2+}]$. Rose (1968) subsequently used this observation to estimate $[Mg^{2+}]$ in

Table 1. Ionization and Stability Constants*

Type	Reaction	K_i	pK_i	Source
Protonated species	$HATP^{3-} \rightleftarrows ATP^{4-} + H^+$	K_{HATP}	6.90	Melchior, 1954
	$HADP^{2-} \rightleftarrows ADP^{3-} + H^+$	K_{HADP}	6.61	Weitzel and Spehr, 1958
	$HAMP^- \rightleftarrows AMP^{2-} + H^+$	K_{HAMP}	6.31	Taqui Khan and Martell, 1967
	$HAc^0 \rightleftarrows Ac^- + H^+$	K_{HAc}	4.64	Feldman and Koval, 1963
	$HAcP^- \rightleftarrows AcP^{2-} + H^+$	K_{HAcP}	4.40	Jencks, 1969
	$H_2ATP^{2-} \rightleftarrows HATP^{3-} + H^+$	K_{H2ATP}	4.06	Taqui Khan and Martell, 1962
	$H_2ADP^- \rightleftarrows HADP^{2-} + H^+$	K_{H2ADP}	3.93	Martell and Schwarzenbach, 1956
	$H_2AMP^0 \rightleftarrows HAMP^- + H^+$	K_{H2AMP}	3.74	Sigel et al., 1967
Mg^{2+} complexes	$MgATP^{2-} \rightleftarrows ATP^{4-} + Mg^{2+}$	K_{MgATP}	4.00	Martell and Schwarzenbach, 1956
	$MgADP^- \rightleftarrows ADP^{3-} + Mg^{2+}$	K_{MgADP}	3.01	
	$MgAMP^0 \rightleftarrows AMP^{2-} + Mg^{2+}$	K_{MgAMP}	1.69	
	$MgAcP^0 \rightleftarrows AcP^{2-} + Mg^{2+}$	K_{MgAcP}	1.48	Satchell and White, 1970
	$MgAc^+ \rightleftarrows Ac^- + Mg^{2+}$	K_{MgAc}	1.28	Archer and Monk, 1964
	$MgOH^+ \rightleftarrows OH^- + Mg^{2+}$	K_{MgOH}	2.60	Stock and Davies, 1948
	$MgCl^+ \rightleftarrows Cl^- + Mg^{2+}$	K_{MgCl}	0.53	Blair, 1970
	$Mg_2ATP^0 \rightleftarrows MgATP^{2-} + Mg^{2+}$	K_{Mg2ATP}	1.30	Burton, 1959
	$Mg(ATP)_2^{6-} \rightleftarrows MgATP^{2-} + ATP^{4-}$	K_{MgATP_2}	2.40	Burton, 1959
Protonated Mg^{2+} complexes	$MgHATP^- \rightleftarrows HATP^{3-} + Mg^{2+}$	K_{MgHATP}	2.70	O'Sullivan and Perrin, 1964
	$MgHADP^0 \rightleftarrows HADP^{2-} + Mg^{2+}$	K_{MgHADP}	1.45	Martell and Schwarzenbach, 1956
Monovalent metal ion complexes	$LiATP^{3-} \rightleftarrows ATP^{4-} + Li^+$	K_{LiATP}	1.57	*Smith* and Alberty, 1956
	$NaATP^{3-} \rightleftarrows ATP^{4-} + Na^+$	K_{NaATP}	1.16	
	$LiADP^{2-} \rightleftarrows ADP^{3-} + Li^+$	K_{LiADP}	1.15	
	$KATP^{3-} \rightleftarrows ATP^{4-} + K^+$	K_{KATP}	1.06	
	$NaADP^{2-} \rightleftarrows ADP^{3-} + Na^+$	K_{NaADP}	0.83	
	$LiAMP^- \rightleftarrows AMP^{2-} + Li^+$	K_{LiAMP}	0.61	
	$KADP^{2-} \rightleftarrows ADP^{3-} + K^+$	K_{KADP}	0.60	
	$NaAMP^- \rightleftarrows AMP^{2-} + Na^+$	K_{NaAMP}	0.45	
	$KAMP \rightleftarrows AMP^{2-} + K^+$	K_{KAMP}	0.20	

* Constants defined in terms of molar concentrations for dissociation reaction as written. Measurements made at 25°C in the presence of noninteracting supporting electrolyte with total ionic strength of 0.1 or 0.2.

red blood cells. Alberty (1969) presented a general theoretical framework and calculated thermodynamic quantities for several reactions involving adenosine phosphates, including reaction (1). His analysis incorporated multiple equilibria between the partially protonated species and Mg^{2+} complexes most likely to form in aqueous solution. More recent studies (Blair, 1970; Horn et al., 1971; DeWeer and Lowe, 1973) have been concerned with fitting ionization and stability constraints to experimental data for K_{1obs} by comparison with theoretical prediction. The constants so obtained differ significantly between investigators. Reaction (2) has received far less attention, the only values of K_{2obs} existing being the few measurements of Rose et al. (1954) which ranged from about 80 to 160. All previous studies of observed equilibrium constants have been carried out with very low concentrations of nucleotides and with ionic strength kept constant at a low value or varied over a narrow range, whereas ionic strength and nucleotide concentrations are likely to be high in a commercial process. Determination of the equilibrium composition of a reaction system for ATP regeneration from AMP or ADP has not previously been examined.

THEORY

The analysis developed here is for a chemical system which may contain the reactants and products of reactions (1) and (2), magnesium ions, monovalent metal ions (Na^+, Li^+, and/or K^+), chloride ions, and a buffer. Table 1 lists the various complexes which may form, as well as the values we have selected for their associated ionization or stability constants. In what follows, the activity of each species is taken to be equal to its molar concentration. Superscripted quantities refer to the concentration of a specific species; absence of a superscript refers to the concentration of a compound in all forms.

In addition to reactions (1) and (2), the following reactions occur:

$$H_2O \rightleftarrows OH^- + H^+ \tag{5}$$

$$HA^{(\nu-1)-} \rightleftarrows A^{\nu-} + H^+ \tag{6}$$

for which the equilibrium constants are

$$K_w = (OH^-)(H^+) \tag{7}$$

$$K_B = \frac{[A^{\nu-}][H^+]}{[HA^{(\nu-1)-}]} \tag{8}$$

Depending upon whether the buffer is a weak acid or a weak base, $HA^{(\nu-1)-}$ and $A^{\nu-}$ may be taken to be a weak acid-conjugate base pair or a conjugate acid-weak base pair, respectively.

We chose as reference species the reactants and products in their totally dissociated forms (Alberty, 1969). The reference reactions are therefore

$$AMP^{2-} + ATP^{4-} \rightleftarrows 2\,ADP^{3-} \tag{9}$$

$$ADP^{3-} + AcP^{2-} \rightleftarrows ATP^{4-} + Ac^- \tag{10}$$

with equilibrium constants

$$K_a = \frac{[ADP^{3-}]^2}{[AMP^{2-}][ATP^{4-}]} \tag{11}$$

$$K_b = \frac{[ATP^{4-}][Ac^-]}{[ADP^{3-}][AcP^{2-}]} \tag{12}$$

K_a is taken to be 2.75 (Alberty, 1969); a value for K_b has not been reported and is to be fitted to our data. Equations (3) and (4) can then be expressed as

$$\frac{[ADP]^2}{[ATP][AMP]} = K_a \frac{f_{ATP} f_{AMP}}{f^2_{ADP}} \tag{13}$$

$$\frac{[ATP][Ac]}{[ADP][AcP]} = K_b \frac{f_{ADP} f_{AcP}}{f_{ATP} f_{Ac}} \tag{14}$$

where f_X is the fraction of component X in its totally dissociated form. For example, if all complexes in Table 1 are assumed to form, then

$$\begin{aligned} f_{ATP} &= [ATP^{4-}]/[ATP] \\ &= [ATP^{4-}]/\{[ATP^{4-}] + [HATP^{3-}] \\ &\quad + [H_2ATP^{2-}] + [MgATP^{2-}] + [MgHATP^-] \\ &\quad + [Mg_2ATP^0] + 2[Mg(ATP)_2^{6-}] + [LiATP^{3-}] \\ &\quad + [NaATP^{3-}] + [KATP^{3-}]\} \\ &= \left\{ 1 + \frac{[H^+]}{K_{HATP}} + \frac{[H^+]^2}{K_{HATP}K_{H2ATP}} + \frac{[Mg^{2+}]}{K_{MgATP}} \right. \\ &\quad + \frac{[Mg^{2+}][H^+]}{K_{HATP}K_{MgHATP}} + \frac{[Mg^{2+}]^2}{K_{MgATP}K_{Mg2ATP}} \\ &\quad + 2\frac{[Mg^{2+}][ATP]f_{ATP}}{K_{MgATP}K_{MgATP_2}} + \frac{[Li^+]}{K_{LiATP}} \\ &\quad \left. + \frac{[Na^+]}{K_{NaATP}} + \frac{[K^+]}{K_{KATP}} \right\}^{-1} \end{aligned} \tag{15}$$

In addition to the equilibrium constraints, the following conservation relations must be enforced:

Adenosine

$$[A] = [AMP] + [ADP] + [ATP] \tag{16}$$

Organic phosphate

$$[P] = [AMP] + 2[ADP] + 3[ATP] + [AcP] \tag{17}$$

Acetate

$$[B] = [AcP] + [Ac] \tag{18}$$

Magnesium

$$\begin{aligned} [Mg] = [Mg^{2+}] \Bigg\{ & 1 + [ATP]f_{ATP}\left(\frac{1}{K_{MgATP}} \right. \\ & + \frac{[H^+]}{K_{HATP}K_{MgHATP}} + \frac{2[Mg^{2+}]}{K_{MgATP}K_{Mg2ATP}} \\ & \left. + \frac{[ATP][f_{ATP}]}{K_{MgATP}K_{MgATP_2}} \right) + [ADP]f_{ADP}\left(\frac{1}{K_{MgADP}} \right. \\ & \left. + \frac{[H^+]}{K_{HADP}K_{MgHADP}} \right) + \frac{[AMP]f_{AMP}}{K_{MgAMP}} + \frac{[AcP]f_{AcP}}{K_{MgAcP}} \\ & + \frac{[Ac]f_{Ac}}{K_{MgAc}} + \frac{[Cl]^-}{K_{MgCl}} + \frac{K_w}{[H^+]K_{MgOH}} \Bigg\} \end{aligned} \tag{19}$$

Monovalent metal ions (M = Li, Na, and/or K)

$$\begin{aligned} [M] = [M^+] \Bigg\{ & 1 + \frac{[ATP]f_{ATP}}{K_{MATP}} \\ & + \frac{[ADP]f_{ADP}}{K_{MADP}} + \frac{[AMP]f_{AMP}}{K_{MAMP}} \Bigg\} \end{aligned} \tag{20}$$

Chloride

$$[Cl] = [Cl^-]\left\{ 1 + \frac{[Mg^{2+}]}{K_{MgCl}} \right\} \tag{21}$$

Buffer

$$[W] = [HA^{(\nu-1)-}] + [A^{\nu-}] \tag{22}$$

Electrical charge

$$\sum_i z_i[i] = 0 \quad i = \text{all charged species} \tag{23}$$

It is assumed in the above development that no compound is hydrolyzed or otherwise degraded.

The solution to Equations (7), (8), (13), (14), and (16) to (23) yields the total concentration of each reactant and product and the concentration of each free ion, from which K_{1obs}, K_{2obs}, and the distribution of individual species may be calculated. In most cases of practical interest, $[H^+]$ can be measured directly and specified as desired by addition of acid or base. In that event, Equations (7), (8), (22), and (23) may be ignored. If either reaction (1) or (2) occur alone, only the appropriate equilibrium relation, Equation (13) or (14), is retained, and the remaining equations are modified to eliminate species not present in solution.

We take the standard set of partially ionized and partially complexed species to be all those listed in Table 1 except for the monovalent metal ion complexes and $MgOH^+$, $MgCl^+$, Mg_2ATP^o, and $Mg(ATP)_2^{6-}$. Inclusion of the latter three compounds (the existence of which is questionable) in the model is considered separately. The problem then reduces to solving for $[Mg^{2+}]$ and the total concentration of reactants and products from Equations (13), (14), and (16) to (19) with the appropriate terms deleted. If, in addition, $[Mg^{2+}]$ is taken to be specified, K_{1obs} and K_{2obs} can be evaluated explicitly from Equations (3), (4), (13), and (14), and the solution is given implicitly by

$$\left\{ \frac{\theta_{ATP}[B]/[A]}{\theta_{ATP} + K_{2obs}\theta_{ADP}} \right\} + 3\theta_{ATP} + 2\theta_{ADP} - \frac{[P]}{[A]} + \left\{ \frac{\theta^2_{ADP}}{K_{1obs}\theta_{ATP}} \right\} = 0 \tag{24}$$

$$\theta_{ADP} = \frac{1}{2}\left\{ -K_{1obs}\theta_{ATP} + [K^2_{1obs}\theta^2_{ATP} - 4(\theta_{ATP} - 1)\theta_{ATP}K_{1obs}]^{1/2} \right\} \tag{25}$$

with

$$\theta_{AMP} = 1 - \theta_{ATP} - \theta_{ADP} \tag{26}$$

$$[AcP] = \frac{[B]}{1 + \dfrac{K_{2obs}\theta_{ADP}}{\theta_{ATP}}} \tag{27}$$

$$[Ac] = [B] - [AcP] \tag{28}$$

where θ_{AXP} is the fraction of total adenosine in the form of the nucleotide AXP. If reaction (2) occurs alone, the last term in braces of Equation (24) is deleted, as is Equation (26). With reactants in stoichiometric proportion ($[B]/[A] = 1$, $[P]/[A] = 3$)

$$\theta_{ATP} = K^{1/2}_{2obs}/(1 + K^{1/2}_{2obs}) \tag{29}$$

If reaction (1) occurs alone, the first term in braces of Equation (24) is deleted, as are Equations (27) and (28). With reactants in stoichiometric proportion ($[P]/[A] = 2$)

$$\theta_{ATP} = 1/(2 + K^{1/2}_{1obs}) \tag{30}$$

EXPERIMENTAL

Materials

Chemicals, except for common reagents, and enzymes [acetate kinase from *E. coli;* adenylate kinase (myokinase) from rabbit muscle] were obtained from Sigma Chemical Co. Reactants were assayed for purity and were used in the following forms: Na_2H_2ATP, NaH_2ADP, H_2AMP, KLiAcP, NaAc. Magnesium was added as $MgCl_2$. All water was twice distilled, the second time with a Corning model 3B glass still. Solution pH was adjusted by addition of hydrochloric acid or sodium hydroxide and measured with glass electrodes (Radiometer type G202C) using an expanded scale *p*H meter (Radiometer model pHM 26). Several measurements of K_{1obs} were made with unbuffered solutions or with 0.2 M triethanolamine (TEA); all other measurements were made with 0.2 M tris-(hydroxymethyl)aminomethane (Tris), a weak base. High [Na] was achieved by addition of sodium chloride. All experiments were carried out in a controlled temperature water bath at 25°C.

Procedures

Observed equilibrium constants were measured at specified *p*H and varying $[Mg^{2+}]$. Reactions were run in forward and reverse directions with the same values of [A], [B], [P], and [Mg]. To equimolar mixtures of reactants or products was added sufficient enzyme to reach equilibrium in several hours for reaction (1) and in about 10 min for reaction (2) in order to minimize acetyl phosphate hydrolysis. ATP concentration was followed with time (Figure 1). When it became constant, samples were taken for quadruplicate analyses of ATP, ADP, AMP, and acetyl phosphate. Samples obtained prior to addition of enzyme were also assayed. Acetate was determined by mass balance. Mass balances for adenosine and phosphate were always satisfied to within ±3%, and observed equilibrium constant measurements were reproducible to within ±5%.

Nucleotide concentration measurements were also made in two series of experiments with ATP regeneration from ADP or AMP. The initial concentration of ADP or AMP was held constant, while the initial concentration of acetyl phosphate was varied. When we began with AMP, a trace amount of ATP was added to start the adenylate kinase reaction.

Analyses

Nucleotide concentration measurements were made with enzymatic assays. Prior to analysis, acetate kinase was irreversibly deactivated by acidification to *p*H < 2. Since adenylate kinase would reactivate upon neutralization during the assay reactions, the system was quenched when it was present by adding 0.2 ml of sample to 5 ml of 0.1 N hydrogen chloride containing 0.5% (w/v) diatomaceous earth (Macaloid, National Lead Co.) which adsorbed all enzyme quantitatively. The preparation was centrifuged, and the supernatant was used for analysis.

ATP concentration was measured with the coupled reactions (Williamson and Corkey, 1969)

$$\text{ATP} + \text{Glucose} \xrightarrow{\text{Hexokinase}} \text{ADP} + \text{Glucose-6-phosphate} \tag{31}$$

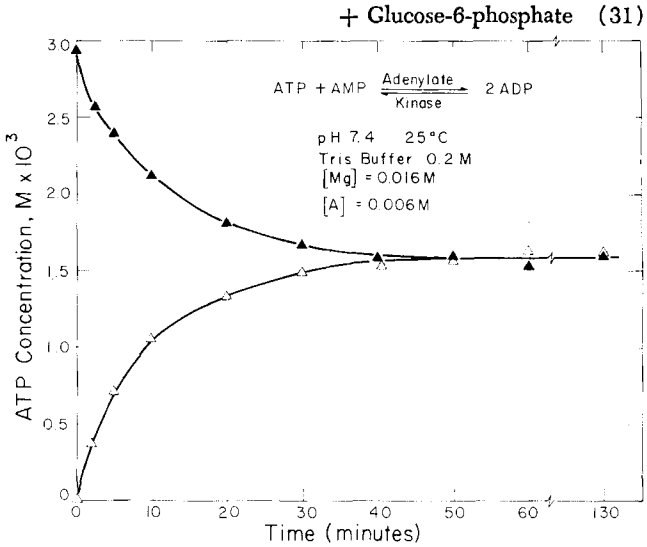

Fig. 1. Typical approach to equilibrium for measurement of K_{1obs} in the forward (▲) and backward (△) directions.

$$NADP^+ + \text{Glucose-6-phosphate} \xrightarrow[\text{Dehydrogenase}]{\text{Glucose-6-phosphate}} \text{6-Phosphogluconate} + NADPH + H^+ \quad (32)$$

To 5 ml ATP assay solution [3.3 mmoles glucose, 0.125 mmoles nicotinamide adenine dinucleotide phosphate ($NADP^+$), 1 250 units hexokinase, and 625 units glucose-6-phosphate dehydrogenase made up to 500 ml with 0.2 M Tris, *p*H 7.4, containing 10 mM $MgCl_2$; stored up to 1 week at 4°C] was added 0.2 ml acidified sample. Reactions (31) and (32) proceeded essentially to completion. Final NADPH concentration (measured spectrophotometrically at 340 nm) equaled the original ATP concentration.

ADP concentration was measured with the coupled reactions (Bernt and Bergmeyer, 1963)

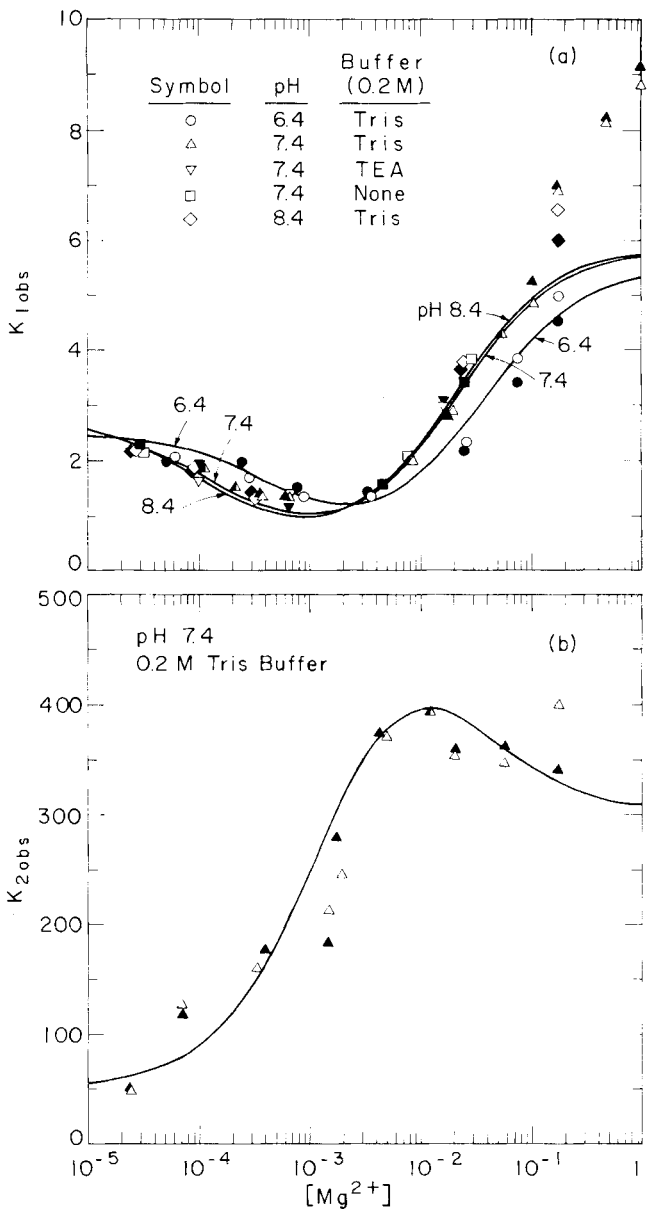

Fig. 2. Observed equilibrium constants measured at 25°C for the reactions catalyzed by (a) adenylate kinase with [A] = 30 mM, [P] = 60 mM; and (b) acetate kinase with [A] = 15 mM, [B] = 15 mM, [P] = 45 mM. Solid curves represent theoretical prediction with standard set of complexes. Open symbols: forward direction; closed symbols: backward direction; half-filled symbols: both directions. Minimum ionic strength was about 0.11 (unbuffered) and 0.18 (buffered); it increased to about 0.55 at $[Mg^{2+}] \simeq 0.1$ M, 0.65 to 0.76 at 0.17 M, and 3.2 at 1 M.

$$ADP + \text{phosphoenol pyruvate} \xrightarrow[\text{Kinase}]{\text{Pyruvate}} ATP + \text{pyruvate} \quad (33)$$

$$H^+ + \text{pyruvate} + NADH \xrightarrow[\text{Dehydrogenase}]{\text{Lactate}} \text{lactate} + NAD^+ \quad (34)$$

To 5 ml ADP assay solution [0.02 mmoles phosphoenol pyruvate, 0.013 mmoles nicotinamide adenine dinucleotide (NADH), 2 000 units lactate dehydrogenase, and 750 units pyruvate kinase, made up to 50 ml with 0.2 M Tris, *p*H 9.0, containing 10 mM $MgCl_2$; prepared within 1 hr of use] was added 0.2 ml acidified sample. Reactions (33) and (34) proceeded essentially to completion. The final decrease in NADH concentration (measured spectrophotometrically at 340 nm) equaled the original ADP concentration.

AMP concentration was next determined by adding 10 units adenylate kinase to the ADP assay mixture. Reactions (1), (33), and (34) proceeded to completion. The additional decrease in NADH concentration equaled twice the original AMP concentration. Acetyl phosphate concentration was measured with the hydroxylamine assay as described previously (Gardner et al., 1976).

All absorbance measurements were made with a Gilford model 240 spectrophotometer with rapid sampler and model 410 digital absorbance meter. Each of the assays was reproducible to within less than ±2%. Additional details about experimental techniques are available (Langer, 1974).

RESULTS AND DISCUSSION

Observed Equilibrium Constants

Observed equilibrium constants are shown as a function of $[Mg^{2+}]$ in Figure 2 for the reaction catalyzed by adenylate kinase at *p*H 6.4, 7.4, and 8.4, and for the reaction catalyzed by acetate kinase at *pH* 7.4. Measured K_{1obs} ranged from about 1 to 9 with a minimum at $[Mg^{2+}] \simeq 10^{-3}$; the data were less sensitive to *p*H than to $[Mg^{2+}]$ over the range studied. K_{2obs} ranged from about 50 to 400 with a maximum at $Mg^{2+} \simeq 10^{-2}$.

The theoretical curves in Figure 2 were evaluated for the standard set of complexes. $[Mg^{2+}]$ for each datum point was calculated by numerical solution of the appropriate set of equations using a variation of Newton's method (Mancino, 1966; Robinson, 1966). Three sets of ionization and stability constants have been proposed for the species involved in the adenylate kinase reaction (Alberty, 1969; Blair, 1970; Horn, 1971). The best agreement between data and prediction at *p*H 7.4 and 8.4 was obtained with the constants used by Alberty. Agreement at *p*H 6.4 was markedly improved by selecting from the literature different constants for $HATP^{3-}$, $HADP^{2-}$, $HAMP^-$, and $MgHATP^-$. The largest change was in K_{MgHATP} which was necessary to fit the observed behavior at high $[Mg^{2+}]$. The mean deviation between measurement and prediction of K_{1obs} which resulted with the pK_i values in Table 1 was 9%, whereas mean deviations of 33 and 24% resulted with the constants proposed by Blair and Horn, respectively. The deviation was 5% at *p*H 7.4 and 8.4 but 33% at *p*H 6.4, with the unadjusted constants of Alberty.

From the constants in Table 1, the value of K_b which provided agreement between measured and predicted K_{2obs} was determined for each datum point. The average value, $K_b = 48.0 \pm 9.0$, was used throughout this study. The mean deviation between prediction and data for K_{2obs} was 16%. The effect on K_{1obs} and K_{2obs} of varying the pK_i for the standard set is described in detail elsewhere (Langer, 1974).

Agreement between data and theory in Figure 2 is excellent for $[Mg^{2+}] \leq 0.1$ M. The model predicted

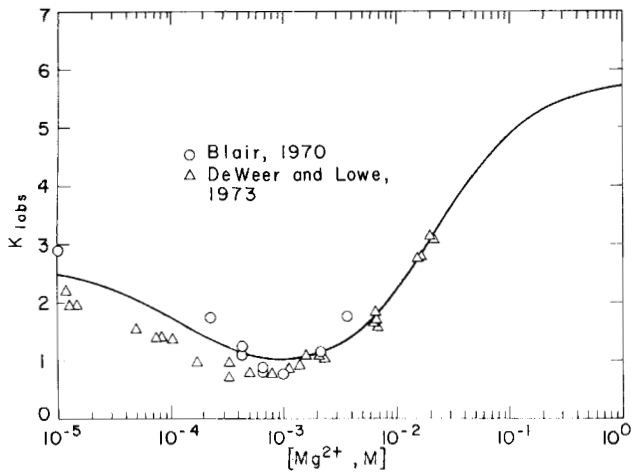

Fig. 3. Comparison between theoretical prediction from this study and observed equilibrium constant data of others for adenylate kinase. Solid curve is for pH 7.4. Data are plotted for $[Mg^{2+}]$ values reported in original studies.

little difference between data for K_{1obs} at pH 7.4 and 8.4, as was observed experimentally. The agreement at pH 7.4 was similar for data obtained in 0.2 M Tris, 0.2 M TEA, and without buffer. This suggests that any complexes formed involving the weak base buffers or their conjugate acids were not significant, as was assumed in the analysis.

In Figure 3 our theoretical prediction of K_{1obs} is compared with experimental data of Blair (1970), obtained at pH 7.25, $I = 0.095$, and of DeWeer and Lowe (1973) obtained at pH 7.5, $I = 0.46$. Comparison is made with the theoretical curve for pH 7.4 which is nearly identical with curves for pH 7.25 and 7.5. The mean deviation between theory and data for all points is 14%.

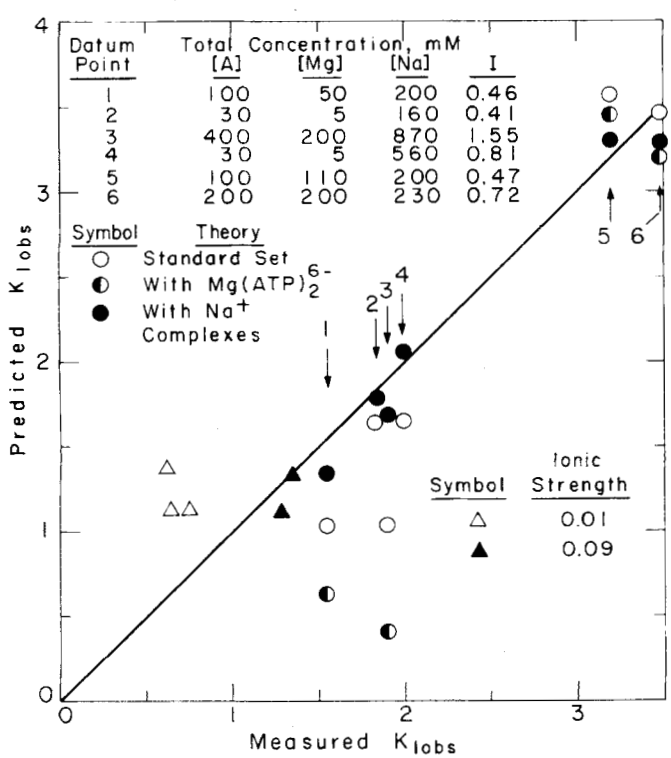

Fig. 4. Comparison between predicted and measured K_{1obs} for (1) experiments in which [A] and/or [Na] was very high and (2) experiments in which ionic strength was very low. K_{1obs} is predicted only with standard set of complexes for low ionic strength data.

Figure 4 compares measured and predicted values of K_{1obs} from two groups of experiments. In the first group, [Na] was kept high, and [A] and [Mg] were varied over a wide range. Each datum point in this group is plotted vs. three values of predicted K_{1obs}. These values were obtained by numerical solution of the appropriate equations for the standard set of complexes, the standard set plus $Mg(ATP)_2^{6-}$, and the standard set plus Na^+ complexes. In the second group of experiments, ionic strength was maintained at much lower levels. Each datum point in this group is plotted vs. predicted K_{1obs} for only the standard set of complexes. For the conditions applicable to Figure 2 ([A] $\leq$ 30 mM, [Na] $\leq$ 45 mM) and to the low ionic strength measurements, inclusion of the other species had negligible effect. With the much higher values of [A] and [Na] in Figure 4, theoretical prediction was improved in all but one case by inclusion of Na^+ complexes, whereas inclusion of $Mg(ATP)_2^{6-}$ substantially increased the deviation between theory and data. Simultaneous inclusion of Na^+ complexes and $(MgATP)_2^{6-}$ led to almost equally poor predicted values (not shown in Figure 4). The results suggest that Na^+ complexes should be incorporated into the model when [Na] $\gtrsim$ 100 mM and when [A] > [Mg] << [Na]. If the last condition is not met, the much greater affinity of Mg^{2+} for the nucleotides prevents significant formation of Na^+ complexes. Since the stability constants for Li^+ and K^+ constants are comparable to those for Na^+, the same guidelines apply. With the levels of Li^+ and K^+ used in this study (<15 mM), their inclusion in the analysis has negligible effect.

The data in Figures 2, 3, and 4 agree well with prediction of the theoretical model over a wide range of

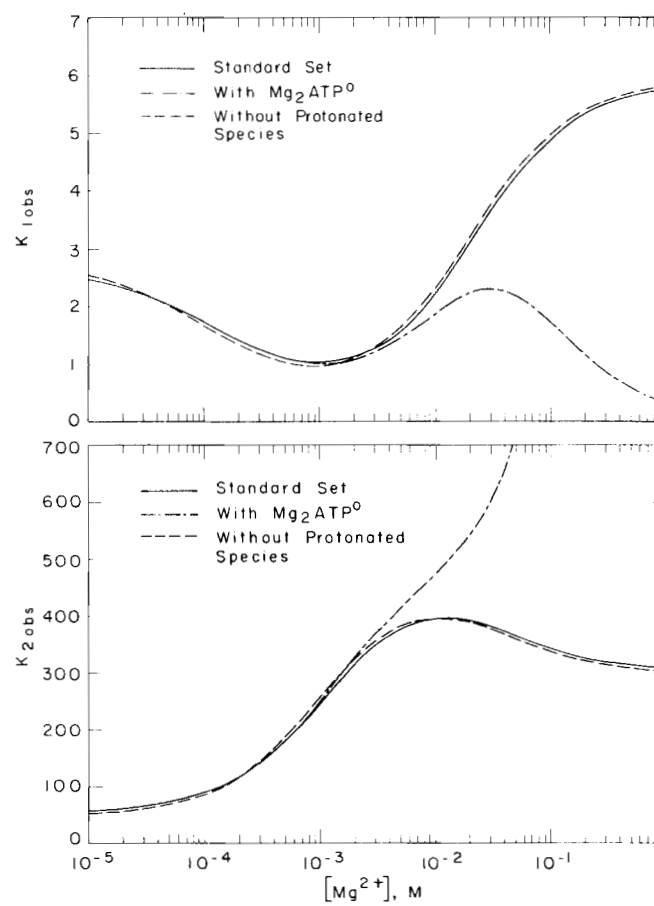

Fig. 5. Effect of (1) including Mg_2ATP^0 and (2) eliminating all protonated species on theoretical predictions of observed equilibrium constants.

conditions ($6.4 \leq pH \leq 8.4$, $0.1 < I < 1.6$, $[Mg^{2+}] < 0.1$ M) which circumscribes the likely range for practical application. The deviation at low ionic strength (Figure 4) is not unexpected, since the effect of ionic strength on the ionization and stability constants defined in terms of concentrations (as in Table 1) is substantial in the range $0 < I < 0.1$ but much smaller for $0.1 \leq I \leq 0.2$ (Phillips et al., 1963, 1966, 1969). The poor agreement for $[Mg^{2+}] > 0.1$ M (Figure 2*a*) may result from some unknown effect specific to Mg^{2+} with the experimental system employed; the effect of increased ionic strength on activity coefficients is unlikely to be the primary cause because good agreement was obtained with ionic strength as high as about 1.6 (Figure 4). Agreement between theory and data over such a large range of conditions is encouraging and may result because activity coefficients of the dominant species change little for $I > 0.1$ or because the changes that do occur compensate for each other.

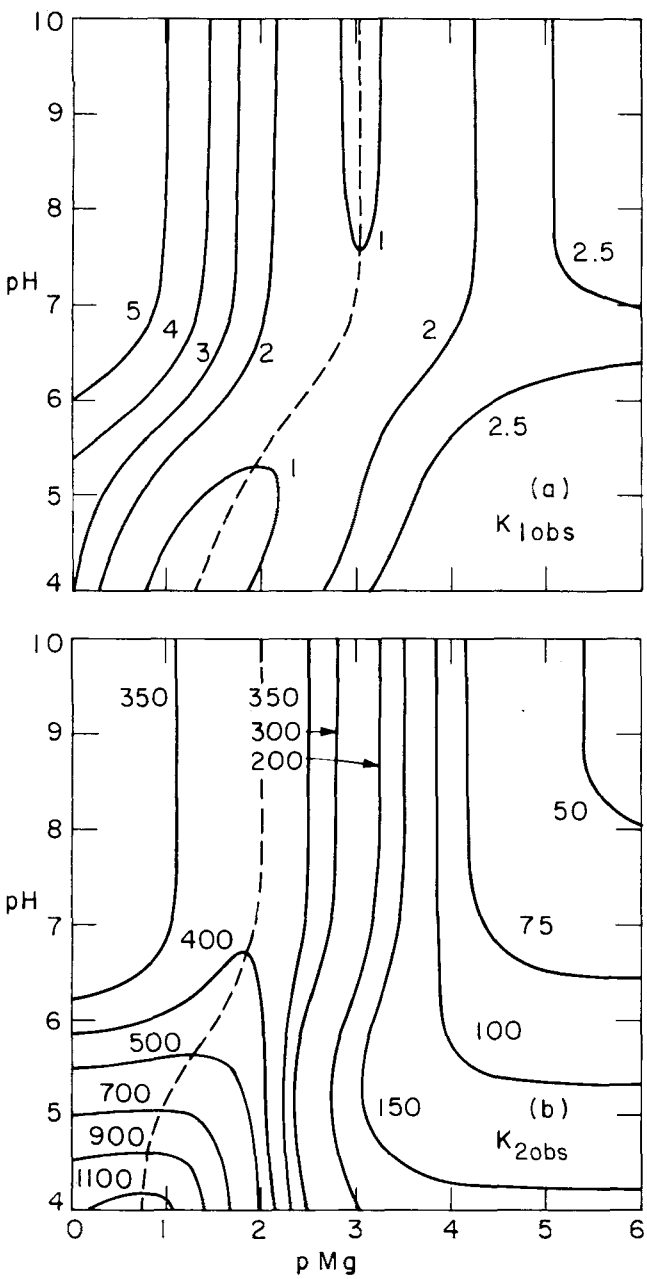

Fig. 6. Contours of constant observed equilibrium constants as a function of pH and pMg for (a) adenylate kinase and (b) acetate kinase. The dashed lines are the loci of points representing a minimum in K_{1obs} and a maximum in K_{2obs}.

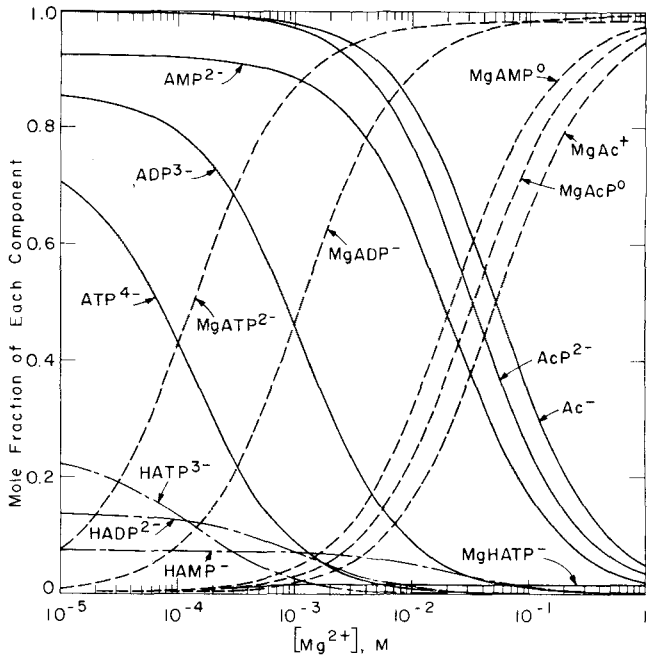

Fig. 7. Distribution of individual species as a function of $[Mg^{2+}]$ at pH 7.4. Calculated with standard set of complexes. Mole fraction refers to individual reactant or product, for example, curve labeled $MgATP^{2-}$ represents $[MgATP^{2-}]/[ATP] = f_{ATP}[Mg^{2+}]/K_{MgATP}$.

The effect of including Mg_2ATP^o in the model is shown in Figure 5. The bimetallic ion complex is predicted to become significant for $[Mg^{2+}] \gtrsim 10^{-3}$ M, but the resulting trend is qualitatively inconsistent with the data in Figure 2. As with $Mg(ATP)_2^{6-}$, evidence for the existence of this species is speculative (Burton, 1959; Kuby and Noltman, 1962; Phillips, 1966; Alberty, 1969), and our results suggest that they do not form. The stability constant for $MgCl^+$ was reported via personal communication (Blair, 1970) without supporting evidence. Its inclusion in the model does not influence theoretical prediction of the observed equilibrium constants, but it does lower the value of $[Mg^{2+}]$ calculated for experimental data points. With respect to the data plotted in Figure 2, the shift of points to the left becomes significant for $[Mg^{2+}] \geq 10^{-2}$ M (Langer, 1974). The major effect of $MgCl^+$ is to make predictions of K_{1obs} worse in the region (pH 7.4, $[Mg^{2+}] > 0.1$ M) where they are already poor, and its inclusion in the model is neither necessary nor desirable. Inclusion of $MgOH^+$ makes no significant difference over the entire range of variables investigated in this study. Therefore, the standard set of complexes suffices for a satisfactory description of the system so long as monovalent ion concentrations are not very high. As shown in Figure 5, all protonated species may be eliminated entirely, while retaining only the Mg^{2+} complexes of the reactants and products, without significant loss of accuracy for prediction of K_{1obs} and K_{2obs} for $pH \geq 7.4$.

The effects of $[H^+]$ and $[Mg^{2+}]$ on observed equilibrium constants are shown over a wide range in Figure 6. The solid curves represent constant values of K_{1obs} or K_{2obs}. Except at high pMg, the results are insensitive to pH for $pH \gtrsim 7$. Figure 6*a* differs from a similar plot by Alberty (1969), especially for $pH < 7$, because of the changes in four dissociation constants. The locus of minima in K_{1obs} occurs at $pMg \simeq 3$ for $pH \gtrsim 7$ but shifts to lower pMg with decreasing pH. The locus of maxima in K_{2obs} occurs at $pMg \simeq 2$ for $pH > 7$ and also shifts to lower pMg with decreasing pH. K_{2obs} is rela-

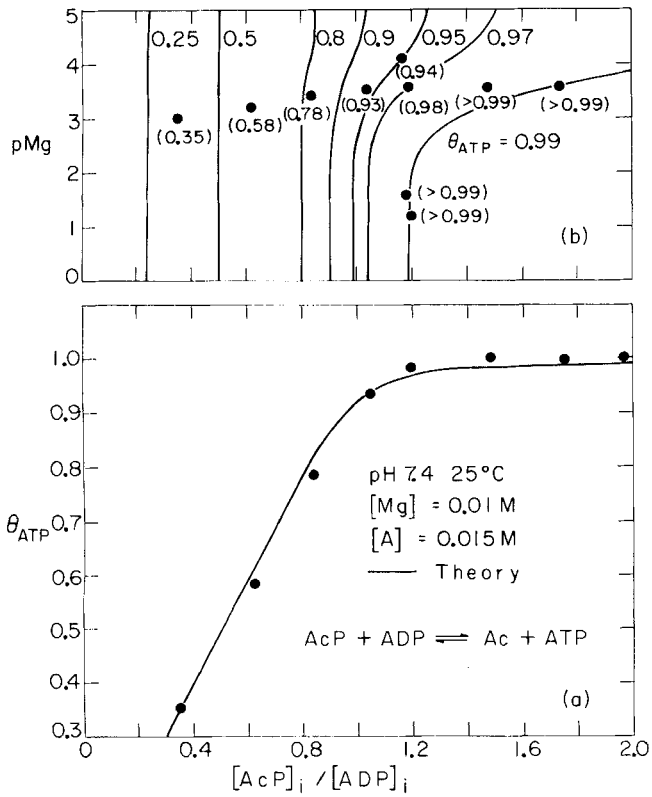

Fig. 8. (a) Dimensionless ATP concentration as a function of reactant ratio for ATP regeneration from ADP. (b) Contour plot for θ_{ATP}. Each number in parentheses is measured θ_{ATP} for the associated datum point from (a). Also plotted are data from several experiments not shown in (a).

tively insensitive to both pH and pMg for $p\text{Mg} \lesssim 3$ and $p\text{H} \gtrsim 7$ but is very sensitive for $p\text{H} \lesssim 7$.

Distribution of Species

The distribution of individual species in solution at pH 7.4 is plotted in Figure 7 as a function of $[Mg^{2+}]$. Totally dissociated anions and Mg^{2+} complexes are the dominant forms. Protonated species, the mole fractions of which are of the order of 0.1 for $[Mg^{2+}] \lesssim 10^{-3}$ M, nevertheless constitute a more significant fraction at pH 7.4 than would be inferred from the effect of deleting protonated species entirely from the model (Figure 5).

These results, and similar plots at lower pH, aid interpretation of Figure 6. In the upper right-hand corner of Figure 6*a*, reaction (9) predominates and $K_{1obs} \simeq K_a$. At the upper left, the predominant reaction is between Mg^{2+} complexes. The minimum in K_{1obs} seen in Figure 6*a* at $[Mg^{2+}] \simeq 10^{-3}$ M, pH $\gtrsim$ 7 occurs when, as shown in Figure 7, most of the AMP is uncomplexed, most of the ATP is complexed by Mg^{2+}, and ADP is split between the two forms. The reaction is then predominantly between the species believed to be kinetically active (Langer, 1974):

$$MgATP^{2-} + AMP^{2-} \rightleftarrows MgADP^{-} + ADP^{3-} \quad (35)$$

with

$$K_a' = \frac{[MgADP^-][ADP^{3-}]}{[MgATP^{2-}][AMP^{2-}]} = \frac{K_a K_{MgATP}}{K_{MgADP}} = 0.281 \quad (36)$$

$[Mg^{2+}]$ is released by the forward reaction at $[Mg^{2+}] \lesssim 10^{-3}$ M, since $y_{ADP} < 1/2(y_{ATP} + y_{AMP})$, whereas $[Mg^{2+}]$ is consumed at $[Mg^{2+}] \gtrsim 10^{-3}$ M since $y_{ADP} > 1/2(y_{ATP} + y_{AMP})$, where y_i is the mole fraction of component i in the form of a Mg^{2+} complex. The increase in K_{1obs} in either direction about the minimum is therefore consistent with Le Chatelier's principle. At the lower left of Figure 6*a*, the species distribution is more complicated because the affinities for Mg^{2+} and H^+ are competitive. The contours are oblique to the coordinates, indicating that Mg^{2+} and H^+ are released or consumed during reaction.

Qualitative trends for the acetate kinase contour plot (Figure 6*b*) are similar. The maximum in K_{2obs} seen in Figure 6*b* at $[Mg^{2+}] \simeq 10^{-2}$ above pH 7 occurs when most of the ADP and ATP are complexed by Mg^{2+}, but most of the AcP and Ac are uncomplexed (Figure 7). These forms represent the presumed kinetically active species (Langer, 1974) which give the reaction

$$MgADP^{-} + AcP^{2-} \rightleftarrows MgATP^{2-} + Ac^{-} \quad (37)$$

with

$$K_b' = \frac{[MgATP^{2-}][Ac^-]}{[MgADP^-][AcP^{2-}]} = K_b \frac{K_{MgADP}}{K_{MgATP}} = 469 \quad (38)$$

Since Mg^{2+} is consumed ($y_{ATP} + y_{Ac} > y_{ADP} + y_{AcP}$) at lower $[Mg^{2+}]$, and the reverse is true at higher $[Mg^{2+}]$, Le Chatelier's principle ensures that the locus of points representing zero production of $[Mg^{2+}]$ with reaction is a maximum in K_{2obs}.

Nucleotide Conversion

Figure 8 is a comparison between measured and predicted ATP concentration from experiments with acetate kinase in which ADP and AcP were the initial reactants and the ratio between the two was varied. The upper curve shows how the conversion to ATP is influenced

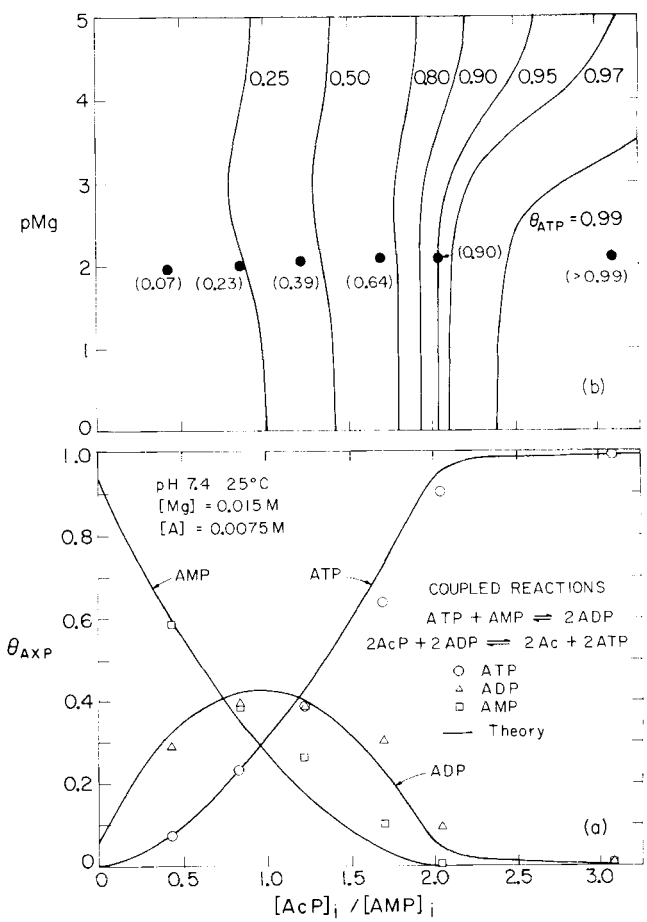

Fig. 9. (a) Total concentration of nucleotides as a function of reactant ratio for ATP regeneration from AMP. (b) Contour plot for θ_{ATP}. Each number in parentheses is measured θ_{ATP} for the associated datum point. $[ATP]_i/[AMP]_i = 0.03$ for both plots.

by $[Mg^{2+}]$ and reactant ratio at pH 7.4. Figure 9 is a similar plot which shows the concentration of each nucleotide for the coupled enzyme system with AMP and AcP as initial reactants (and a small amount of ATP to start the reaction).

In both cases, agreement between prediction and data is satisfactory. Conversion to ATP in excess of 90% with reactants in stoichiometric proportion, and greater than 99% with a 50% molar excess of AcP, was predicted and experimentally achieved. Maximum theoretical conversion at $p\text{H} \geq 7.4$ is 93.3% and 95.2% for regeneration from AMP and ADP, respectively, with stoichiometric reagents and over 99% with about a 20% excess of AcP over stoichiometric. These high conversions for regeneration from AMP are, of course, attained only if the enzymatic reactions are coupled in the same reaction zone.

At low reactant ratios with the coupled system, conversion is most influenced by the adenylate kinase equilibrium and is maximized at $[Mg^{2+}] \simeq 10^{-3}$ M for $p\text{H} \gtrsim 7$ which reflects the minimum in $K_{1\text{obs}}$. At higher reactant ratios, the contours are similar in both Figures 8 and 9 because the acetate kinase equilibrium is more important; the highest conversions are attained with $[Mg^{2+}] \gtrsim 10^{-2}$, where $K_{2\text{obs}}$ is a maximum. The contours in Figure 6*b* suggest that even higher equilibrium conversions are attainable by operation at low pH. However, such low values of pH are not practical because acetate kinase activity drops substantially for $p\text{H} < 6$ (Langer, 1974). The ultimate constraints on the use of reactions (1) and (2) are likely to result from kinetic, as well as equilibrium, phenomena. Kinetic studies with the two enzymes will be discussed in future papers.

ACKNOWLEDGMENT

This work was supported in part by grant GI-34284 from the National Science Foundation. The experimental assistance of Mr. Brian Yorgey and Mr. Morris Kopels is gratefully acknowledged.

NOTATION

A = total adenosine
Ac = acetate
AcP = acetyl phosphate
ADP = adenosine diphosphate
AMP = adenosine monophosphate
ATP = adenosine triphosphate
B = total acetate
f_X = mole fraction of species X in totally dissociated form
I = ionic strength
$K_{1\text{obs}}$ = observed equilibrium constant for adenylate kinase reaction
$K_{2\text{obs}}$ = observed equilibrium constant for acetate kinase reaction
K_B, K_a, K_b, K_w = equilibrium constants defined by Equations (7), (8), (11), and (12)
K_a', K_b' = equilibrium constants for reactions between kinetically active species, defined by Equations (36) and (38)
K_i = dissociation constant for species i
M = alkali metal (Li, Na, or K)
NAD^+ = nicotinamide adenine dinucleotide (oxidized form)
NADH = nicotinamide adenine dinucleotide (reduced form)
$NADP^+$ = nicotinamide adenine dinucleotide phosphate (oxidized form)
NADPH = nicotinamide adenine dinucleotide phosphate (reduced form)
$p\text{Mg}$ = $-\log[Mg^{2+}]$, defined analogously to $p\text{H}$, pK_i
P = total organic phosphate
W = total buffer
y_i = mole fraction of component i in the form of a Mg^{2+} complex
z_i = electrical charge on species i
θ_{ATP} = [AXP]/[A], fraction of total adenosine in the form of AXP

LITERATURE CITED

Alberty, R. A., "Standard Gibbs Free Energy, Enthalpy, and Entropy Changes as a Function of pH and pMg for Several Reactions Involving Adenosine Phosphates," *J. Biol. Chem.*, **244**, 3290 (1969).

Archer, D. W., and C. B. Monk, "Ion-association Constants of Some Acetates by pH (Glass Electrode) Measurements," *J. Chem. Soc.*, 3117 (1964).

Bernt, E., and H. Bergmeyer, "Creatine Phosphokinase," in *Methods of Enzymology*, H. Bergmeyer, ed., Vol. 6, p. 859, Academic Press, New York (1963).

Blair, J. McD., "Magnesium, Potassium and the Adenylate Kinase Equilibrium," *Eur. J. Biochem.*, **13**, 384 (1970).

Bowen, W. J., and T. D. Kerwin, "The Kinetics of Myokinase. II. Studies of Heat Denaturation, the Effects of Salts and the State of Equilibrium," *Arch. Biochem. Biophys.*, **64**, 278 (1956).

Burton, K., "Formation Constants for the Complexes of Adenosine Di- or Triphosphate with Magnesium or Calcium Ions," *Biochem. J.*, **71**, 388 (1959).

DeWeer, P., and A. G. Lowe, "Myokinase Equilibrium," *J. Biol. Chem.*, **248**, 2829 (1973).

Feldman, I., and L. Koval, "Reaction of the Uranyl Ion with Amino Acids. Bidentate Carboxylate Chelation," *Inorganic Chem.*, **2**, 145 (1963).

Gardner, C. R., R. S. Langer, and C. K. Colton, "Dependence on pH of the Hydroxylamine Assay for Acyl Phosphates," *Anal. Biochem.* (1976, in press).

Horn, A., R. Husung, M. Schroeder, and H. Boernig, "The Equilibrium of Adenylate Kinase as a Function of the Concentration of Magnesium and Hydrogen Ions," *Acta Biol. Med. Ger.* **27**, 821 (1971).

Jencks, W. P., *Catalysis in Chemistry and Enzymology*, p. 583, McGraw-Hill, New York (1969).

Kuby, S. A., and E. A. Noltman, "ATP-Creatine Transphosphorylase," in *The Enzymes*, P. Boyer, ed., Vol. 6, p. 515, Academic Press, New York (1962).

Langer, R. S., "Enzymatic Regeneration of ATP," Sc.D. thesis, Mass. Inst. Technol., Cambridge (1974).

Langer, R. S., B. K. Hamilton, C. R. Gardner, M. C. Archer, and C. K. Colton, "Enzymatic Regeneration of ATP. I. Alternative Routes," *AIChE J.*, **22**, 1079 (1976).

Mancino, O. G., "Resolution by Iteration of Some Nonlinear Systems," *J. Assoc. Computing Machinery*, **14**, 341 (1966).

Martell, A. E., and G. Schwarzenbach, "Adenosinephosphate und Triphosphat als Komplex bildner für Calcium und Magnesium," *Helv. Chim. Acta*, **39**, 653 (1956).

Melchior, N. C., "Sodium and Potassium Complexes of Adenosine Triphosphate: Equilibrium Studies," *J. Biol. Chem.*, **208**, 615 (1954).

O'Sullivan, W. J., and D. D. Perrin, "The Stability Constants of Metal-Adenine Nucleotide Complexes," *Biochem.*, **3**, 18 (1964).

Phillips, R., "Adenosine and the Adenine Nucleotides. Ionization, Metal Complex Formation, and Conformation in Solution," *Chem. Rev.*, **66**, 501 (1966).

Phillips, R. C., P. George, and R. J. Rutman, "Potentiometric Studies of the Secondary Phosphate Ionizations of AMP, ADP, and ATP, and Calculations of Thermodynamic Data for the Hydrolysis Reactions," *Biochem.*, **2**, 501 (1963).

———, "Thermodynamic Studies of the Formation and Ionization of the Magnesium (II) Complexes of ADP and ATP over the pH Range 5 to 9," *J. Am. Chem. Soc.*, **88**, 2631 (1966).

———, "Thermodynamic Data for the Hydrolysis of

Adenosine Triphosphate as a Function of pH, Mg^{2+} Ion Concentration, and Ionic Strength," *J. Biol. Chem.*, **244**, 3330 (1969).
Robinson, S. M., "Interpolative Solution of Systems of Nonlinear Equations," *SIAM J. Numer. Anal.*, 3, 650 (1966).
Rose, I. A., "The State of Magnesium in Cells as Estimated from the Adenylate Kinase Equilibrium," *Proc. Natl. Acad. Sci.*, **61**, 1079 (1968).
———, M. Grunberg-Manago, S. R. Korey, and S. Ochoa, "Enzymatic Phosphorylation of Acetate," *J. Biol. Chem.*, **211**, 734 (1954).
Satchell, D. P. N., and G. F. White, "Kinetic Studies with Acetate Kinase," *Biochim. Biophys. Acta*, **212**, 248 (1970).
Sigel, H., K. Becker, and D. B. McCormick, "Ternary Complexes in Solution. Influence of 2,2′ Bipyridyl on the Stability of 1:1 Complexes of Co^{2+}, Ni^{2+}, Cu^{2+} and Zn^{2+} with Hydrogen Phosphate, Adenosine 5′-Monophosphate and Adenosine 5′-Triphosphate," *ibid.*, **148**, 655 (1967).
Smith, R. M., and R. A. Alberty, "The Apparent Stability Constants of Ionic Complexes of Various Adenosine Phosphates with Monovalent Cations," *J. Phys. Chem.*, **60**, 180 (1956).
Stock, D. I., and C. W. Davies, "The Second Dissociation Constant of Magnesium Hydroxide," *Trans. Faraday Soc.*, **44**, 856 (1948).
Taqui Khan, M. M., and A. E. Martell, "Metal Chelates of Adenosine Triphosphate," *J. Phys. Chem.*, **66**, 10 (1962).
———, "Thermodynamic Quantities Associated with the Interaction of Adenosinediphosphoric and Adenosinemonophosphoric Acids with Metal Ions," *J. Am. Chem. Soc.*, 89, 5585 (1967).
Weitzel, G., and T. Spehr, "Zinc Complexes of Purines, Nucleosides and Nucleotides," *Z. Physiol. Chem.*, **313**, 212 (1958).
Williamson, J. R., and E. B. Corkey, "Assays of Intermediates of the Citric Acid Cycle and Related Compounds by Fluorometric Enzyme Methods," in *Methods in Enzymology*, S. P. Colowick and N. O. Kaplan, ed., Vol. 3, p. 434, Academic Press, New York (1969).

Manuscript received July 28, and accepted October 8, 1976.

A Comprehensive Correlating Equation for Laminar, Assisting, Forced and Free Convection

STUART W. CHURCHILL

Department of Chemical and Biochemical Engineering
University of Pennsylvania
Philadelphia, Pennsylvania 19174

A correlating equation for assisting convection was developed by combining correlating equations for pure free and pure forced convection. These component equations are based on laminar boundary-layer theory for an isothermal, vertical plate. Theoretical values for assisting convection indicate that the third root of the sum of the third powers gives the best representation, as contrasted with the choice and rationalization of the second or fourth power by prior investigators.

This expression was modified by the addition of a limiting value Nu_0 to obtain a better representation below the domain of boundary-layer theory and was generalized for uniform heating and for spheres and horizontal cylinders by the appropriate choice of the characteristic length.

SCOPE

Heat transfer by forced convection implies a temperature difference and hence a density difference. The density difference gives rise to free convection. This coupled process has been the subject of both experimental and theoretical investigations for a variety of geometries and conditions. A number of different correlating equations have been proposed for particular cases. However, the accuracy, generality, and range of validity of these correlations have not been tested critically.

The objective of this work has been to develop a more general and accurate correlating equation for combined convection. Attention is confined to assisting convection, that is, to forced flow in the same direction as the buoyant motion, and to the laminar regime but includes the effects of the Prandtl number, boundary conditions, and shape.

The correlating equation is based on theoretical results for free convection, forced convection, and combined convection for vertical plates but was tested with experimental data for plates, spheres, and horizontal cylinders.

CONCLUSIONS AND SIGNIFICANCE

Equation (18), together with supplementary Equations (11) and (12) and the coefficients in Table 1, provide a good representation for the experimental data for both the local and overall Nusselt number for combined forced and free convection from a vertical plate over the entire potential flow and laminar boundary-layer regimes ($Re < 10^4$, $Ra < 10^9$) for all Prandtl numbers and for both uniform surface temperature and uniform heating. This expression appears to be valid for spheres and horizontal cylinders if the indicated characteristic lengths are used. It appears to be applicable for other shapes, such as wedges and vertical cylinders, based on the fragmentary values which are available.